Journal of Solid State Chemistry 187 (2012) 269–275

Contents lists available at SciVerse ScienceDirect

Journal of Solid State Chemistry

journal homepage: www.elsevier.com/locate/jssc

The thioantimonate anion SbS_3^{3-} acting as ligand: Syntheses, crystal structures and selected properties of $[Mn(1,2\text{-chxn})_2SbS_3H]$ and $[Cr(1,3\text{-dap})_2SbS_3]$

B. Seidlhofer, V. Spetzler, C. Näther, W. Bensch *

Institut für Anorganische Chemie, Christian-Albrechts-Universität Kiel, Max-Eyth-Str. 2, D-24118 Kiel, Germany

ARTICLE INFO

Article history:
Received 23 September 2011
Received in revised form
5 January 2012
Accepted 8 January 2012
Available online 20 January 2012

Keywords:
Solvothermal synthesis
Thioantimonate(III)
Thermal stability
Crystal Structure

ABSTRACT

Two new isolated thioantimonates $[Mn(1,2\text{-chxn})_2SbS_3H]$ (**1**) (1,2-chxn=1,2-diaminocyclohexane) and $[Cr(1,3\text{-dap})_2SbS_3]$ (**2**) (1,3-dap=1,3-diaminopropane) were synthesized under solvothermal conditions. The crystal structures of **1** and **2** consist of neutral Mn^{2+} or Cr^{3+} complexes with the transition metal cations being in a distorted octahedral environment of four nitrogen atoms of 1,2-chxn resp. 1,3-dap and two sulphur atoms of the bidentate SbS_3^{3-} unit. Compound **1** is remarkable because charge neutrality is achieved by the presence of Mn^{2+} and a SH group which was never observed before. In both compounds intermolecular S···H bonding interactions connect the complexes into higher dimensionality. Compound **1** crystallizes in the monoclinic space group $P2_1/c$ with $a=21.5440(16)$ Å, $b=6.9295(3)$ Å, $c=13.9276(10)$ Å and $\beta=102.692(8)^\circ$. Compound **2** crystallizes in the orthorhombic space group *Pbca* with $a=8.5999(2)$, $b=15.9741(4)$ and $c=21.6770(7)$ Å.

1. Introduction

The solvothermal synthesis of thiometallates is explored since nearly 40 years [1–5] and the number of such compounds increased significantly during the last few years. Many different assemblies of the inorganic networks are observed [6–8] but despite the numerous examples only a few synthetic rules of thumb are at hand to plan the preparation of a new compound. Some general observations should be shortly summarized: the inorganic part of a thiometallate compound may consist of isolated anions, chains, two-dimensional sheets or a three-dimensional network [9–23]. Otherwise, many thiometallates may be classified on the basis of the organic part of the structure which is often a protonated amine or a transition metal complex. In both cases the ammonium ion or transition metal complex acts as structure director and charge compensator. In some special cases the transition metal cations have a high tendency to form bonds to the thiometallate networks as exemplified by several Cu(I), Ag(I) and Mn(II) containing compounds [10,11,14,24–38].

The number of isolated thioantimonates where the inorganic part acts as a ligand is limited. Many transition metal cations (TM^{n+}) prefer octahedral or trigonal-bipyramidal geometries and only if tetradentate ligands like tren (tris(2-aminoethyl)amine) or trien (triethylenetetraamine) are applied the favoured coordination is not satisfied offering the possibility of an integration of the transition metal cation into the thioantimonate network [6]. In such cases one or two coordination sites at the TM^{n+} ion are left free for bond formation to S atoms of the thioantimonate anion. Until now, only one isolated thioantimonate compound was reported where the TM^{n+} is coordinated by four N atoms of the bidentate amine en (ethylenediamine) and two S atoms of a SbS_3^{3-} anion, namely $[Cr(en)_2SbS_3]$ [39].

The largest isolated anion $[Mn_2Sb_4S_{12}]^{8-}$ acts as a octadentate ligand to four $[Mn(tren)]^{2+}$ complexes in $[\{Mn(tren)\}_4Mn_2Sb_4S_{12}]$ [35]. The inorganic part contains 4-membered and 6-membered heterocycles which are constructed by interconnection of $[SbS_3]$ pyramids and $[MnS_4]$ tetrahedra. In $[\{Mn(tren)\}_2Mn_2Sb_4S_{10}]$ [10] the tetradentate anion $[Mn_2Sb_4S_{10}]^{4-}$ is bound to two manganese complexes. The main structural motif is a $Mn_2Sb_2S_4$ ring being joined to the $[Mn(tren)]^{2+}$ complexes by four Sb_2S_2 rings. Three different compounds with an $[Sb_4S_8]^{4-}$ ligand are known: $[\{Co(tren)\}_2Sb_4S_8]$ [40], $[\{Zn(tren)\}_2Sb_4S_8]$–$0.75H_2O$ [41] and $\{[In(trans\text{-}1,2\text{-chxn})_2]_2Sb_4S_8\}Cl_2$ (*trans*-1,2-chxn=*trans*-1,2-diaminocyclohexane) [42]. The ligand is composed of $[SbS_3]$ and $[SbS_4]$ units sharing two edges with each other in the first two compounds. In $\{[In(1,2\text{-chxn})_2]_2Sb_4S_8\}Cl_2$ the $[Sb_4S_8]^{4-}$ anion acts as a tetradentate ligand and joins two symmetry related In^{3+} centered complexes. Such a binding mode was never observed before for the $[Sb_4S_8]^{4-}$ anion. A $[CoS_4]$ tetrahedron is edge-linked to two $[SbS_3]$ pyramids forming the core in $[\{Co(tren)\}_2CoSb_2S_6]$ [43].

* Corresponding author. Fax: +49 0431 8801520.
E-mail address: wbensch@ac.uni-kiel.de (W. Bensch).

0022-4596/$ - see front matter © 2012 Elsevier Inc. All rights reserved.
doi:10.1016/j.jssc.2012.01.013

The $[Sb_2S_5]^{4-}$ anion in $[\{Mn(tren)\}_2Sb_2S_5]$ is tetradentate and is constructed by two SbS_3 pyramids sharing one edge [10]. A different binding mode can be observed in $[\{Co(tren)\}_2Sb_2S_5]$ [40]. The $[Sb_2S_5]^{4-}$ anion being composed of two edge-linked $[SbS_3]$ pyramids acts in a bidentate mode to two $[Co(tren)]^{2+}$ complexes. Finally, three charge neutral complexes with a bidentate acting $[SbS_3]^{3-}$ anion are known: $[Cr(en)_2SbS_3]$, $[Cr(tren)_2SbS_3]$ and $[Cr(trien)_2SbS_3]$ [9,39,44] which all contain the Cr^{3+} cation.

Only a few isolated thioantimonates(V) containing transition metal cations coordinated by N and S atoms were reported: $[Co(dien)_2][Co(tren)SbS_4]_2 \cdot 4H_2O$ (dien=diethylenetriamine) [45], [Ni(tren)SbS_4](paH) (pa=propylamine) [46], [Mn(tren)(trenH)SbS_4] and $[Mn(trans\text{-}1,2\text{-chxn})_3]_2[Mn(trans\text{-}1,2\text{-chxn})_2(SbS_4)_2]\text{–}6H_2O$ [34]. The $[SbS_4]^{3-}$ anion acts a monodentate ligand or bidentate in [Ni(tren)SbS_4](paH) [46].

In this work we report two new thioantimonates where the transition metal is coordinated by both an organic and inorganic ligand: $[Mn(1,2\text{-chxn})_2SbS_3H]$ (**1**) and $[Cr(1,3\text{-dap})_2SbS_3]$ (1,3-dap=1,3-diaminopropane) (**2**). Compound **1** is the first example for the successful covalent bond formation between Mn^{2+} and the smallest isolated thioantimonate(III) anion.

2. Experimental section

2.1. Synthesis

Both compounds were prepared under solvothermal conditions. Steel autoclaves with Teflon liners of 30 mL volume were used as reaction vessels. Compound **1** was obtained by reacting 1 mmol Sb, 1.5 mmol Mn and 4 mmol S in 3 mL 100% *trans*-1,2-diaminocyclohexane for 7 days at 130 °C. Yellow crystals were obtained in a yield around 40% based on Sb and were washed with water and acetone. Dark red crystals of **2** could be synthesized from a mixture of 0.5 mmol Sb_2S_3, 1.3 mmol S and 0.7 mmol $CrCl_3 \cdot 6H_2O$ in 5 mL 1,3-diaminopropane heated for 7 days at 130 °C. The crystals were washed with water and acetone. The yield of the product was about 80% based on antimony.

Elemental analysis **1**: found: C 28.72%, H 5.81%, N 11.32%; calc.: C 28.70%, H 5.82%, N 11.15%; **2**: found: C 16.67%, H 4.56%, N 12.66%; calc.: C 17.23%, H 4.82%, N 13.40%. EDX measurements **1** found: Mn 20.66%, S 35.48%, Sb 43.86%; calc.: Mn 20.13%, S 35.25%, Sb 44.62%; **2**: found: Cr 18.34%, S 35.98%, Sb 45.67%; calc.: Cr 19.26%, S 35.64%, Sb 45.10%.

2.2. Crystal structure determination

The single crystal X-ray intensity data of **1** were collected at 170 K and of **2** at room temperature on an IPDS-1 (**1**) or IPDS-2 (**2**) Imaging Plate Diffraction System from STOE & Cie with graphite monochromated MoK_α radiation. Selected crystal data and details of the structure determination are summarised in Table 1. The raw intensities were corrected for Lorenz and polarisation effects. A numerical absorption correction was performed for both compounds. The structures were solved with direct methods using SHELXS-97 [47] and the refinement was performed against F^2 using SHELXL-97 [48]. All non-hydrogen atoms except disordered C atoms were refined using anisotropic displacement parameters. The H atoms were positioned with idealised geometry and refined isotropically using a riding model. Crystallographic data have been deposited with the Cambridge Crystallographic Data Centre (CCDC ID: 861409 and 861410). Copies of the data may be obtained free of charge on application to CCDC, 12 Union Road, Cambridge CB2 1E2, U.K. (fax int. code +(44)01223/336033 or e-mail: deposit@chemcrys.cam.ac.uk).

Table 1
Selected crystal data and refinement results for compounds **1**–**2**.

Compound	**1**	**2**
Crystal system	$[Mn(1,2\text{-chxn})_2SbS_3H]$	$[Cr(1,3\text{-dap})_2SbS_3]$
a (Å)	Monoclinic	Orthorhombic
b (Å)	21.5440(16)	8.5999(2)
c (Å)	6.9295(3)	15.9741(4)
α (°)	13.9276(10)	21.6770(7)
β (°)	90	90
γ (°)	102.692(8)	90
V (Å^3)	90	90
Space group	2028.4(2)	2,977.89(14)
Z	$P2_1/c$	$Pbca$
Calc. density (g cm^{-3})	4	4
Crystal color	1.645	2.302
μ (mm^{-1})	Yellow	Dark red
Scan range	2.26	4.38
Index range	$2.91 \le \theta \le 28.10$	$1.88 \le \theta \le 29.20$
	$-28 \le h \le 28$	$-11 \le h \le 11$
	$-8 \le k \le 9$	$-21 \le k \le 21$
	$-18 \le l \le 18$	$-29 \le l \le 29$
Reflections collected	18,897	33,442
Independent reflections	4,887	4,002
R_{int}	0.0294	0.0372
Temperature (K)	170	293
Min./max. transmission	0.6666/0.7605	0.5115/0.5866
Refl. with $F_o > 4\sigma(F_o)$	4,194	3,540
Number of parameters	223	136
R_1 for $F_o > 4\sigma(F_o)$	0.0243	0.0442
w$R2$ for all reflections	0.0633	0.1019
GOOF	1.037	1.118
$\Delta\rho$ (eÅ^{-3})	−0.548/0.589	−0.868/0.541

2.3. Thermoanalytical measurements

Thermogravimetric analyses were performed on a Netzsch STA-429 DTA-TG device. All measurements were corrected for buoyancy and current effects and were done with heating rates of 4 K min^{-1} in Al_2O_3 crucibles under dynamic Ar atmosphere with a flow rate of 75 mL min^{-1}.

2.4. Spectroscopy

The Raman spectra were measured from 100 to 3500 cm^{-1} with a Bruker IFS 66 Fourier transform Raman spectrometer with a wavelength of 514.5 nm. The MIR spectrum of compound **1** was recorded between 450 and 3000 cm^{-1} with an ATI Mattson Genesis spectrometer.

2.5. Magnetic measurements

Magnetic susceptibility measurements were performed on a PPMS (Quantum Design) instrument applying 5 T as external field. The experiment was performed in the zero field cooled mode followed by a field cool run (T: 2 to 300 K). Crystals were hand-picked for the measurement but contained some impurities on the surface which could not be removed.

3. Results and discussion

3.1. Crystal structures

Compound **1** crystallizes in the monoclinic space group $P2_1/c$ (Table 1) with 4 formula units per unit cell. All atoms are located on general positions. The crystal structure consists of a neutral Mn complex (Fig. 1) with the Mn^{2+} cation being chelated by two 1,2-chxn molecules and two S atoms of the SbS_3^{3-} anion yielding a

distorted octahedral coordination. The charge neutrality of the complex is achieved by protonation (IR: absorption band at 2464 cm^{-1}) of the S(3) atom [49]. Bond-valence sum calculations yield 1.94 for the Mn centre and 3.37 for the Sb atom with individual values for the Sb–S bonds of 0.89 for Sb–S(3), 1.23 for Sb–S(1) and 1.26 for Sb–S(2). These values are consistent with the charge balance by the thiol-group in compound **1**.

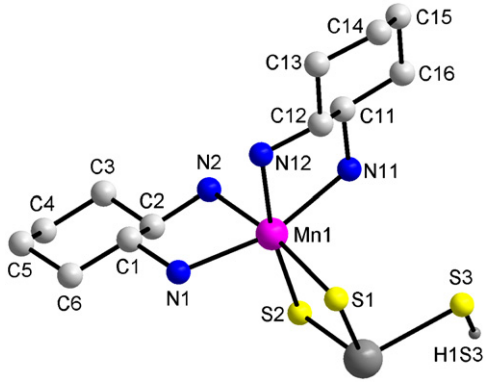

Fig. 1. The $[Mn(1,2\text{-chxn})_2SbS_3H]$ complex (the hydrogen atoms bonded on N and C atoms are omitted for clarity).

Table 2
Bond lengths (Å) and angles (°) for $[Mn(1,2\text{-chxn})_2SbS_3H]$ (1).

Sb(1)–S(1)	2.3677(6)	N(1)–Mn(1)–N(12)	92.21(7)
Sb(1)–S(2)	2.3568(6)	N(1)–Mn(1)–S(1)	98.51(4)
Sb(1)–S(3)	2.5000(7)	N(1)–Mn(1)–S(2)	97.29(5)
S(1)–Mn(1)	2.5844(6)	N(2)–Mn(1)–N(1)	76.10(6)
S(2)–Mn(1)	2.6249(6)	N(2)–Mn(1)–N(11)	92.11(7)
		N(2)–Mn(1)–N(12)	93.01(7)
Mn(1)–N(1)	2.2785(18)	N(2)–Mn(1)–S(1)	171.58(5)
Mn(1)–N(2)	2.2678(17)	N(2)–Mn(1)–S(2)	86.84(5)
Mn(1)–N(11)	2.2691(18)	N(11)–Mn(1)–N(1)	163.00(7)
Mn(1)–N(12)	2.3016(18)	N(11)–Mn(1)–N(12)	75.99(7)
		N(11)–Mn(1)–S(1)	94.48(6)
S(1)–Sb(1)–S(3)	93.67(2)	N(11)–Mn(1)–S(2)	94.19(5)
S(2)–Sb(1)–S(1)	99.308(19)	N(12)–Mn(1)–S(1)	93.67(5)
S(2)–Sb(1)–S(3)	102.45(2)	N(12)–Mn(1)–S(2)	170.17(5)
Sb(1)–S(1)–Mn(1)	86.715(18)	S(1)–Mn(1)–S(2)	87.45(2)
Sb(1)–S(2)–Mn(1)	86.012(19)		

Table 3
Hydrogen bonds of $[Mn(1,2\text{-chxn})_2SbS_3H]$.

D–H		d(H…A)	< DHA/°
S1	H3N	2.5629(1)	174.264(3)
S1	H1S3	2.6185(1)	173.218(1)
S2	H2N	2.5850(1)	161.485(2)

The Mn–S and Mn–N bond lengths as well as the N–Mn–N/N–Mn–S angles are in good agreement with those reported for other Mn thioantimonates (Table 2) [10,11,14,31–38]. The Mn–N(12) bond of 2.3016(18) Å is slightly longer then the other three Mn–N(1, 2, 11) distances (2.2678(3) –2.2785(3) Å). This behaviour may be due to steric constraints of the ligands. The Sb atom is surrounded by 3 S atoms in a trigonal pyramidal coordination which is well known for thioantimonate(III) compounds [10,11,14,31–38]. The Sb–S bonds of 2.3568(6) – 2.5000(7) Å and S–Sb–S angles of 93.67(2)–102.45(2)° (Table 2) are in the range reported for other thioantimonates [10,11,14,31–38]. Generally, the terminal Sb–S bond in isolated thioantimonates is shorter then the bridging bonds [9,39,44]. Interestingly, in **1** the terminal Sb–S(3) bond is longer then the bridging Sb–S(1, 2) bonds which may be caused by the protonation of the S(3) atom.

The bond valence sum for Mn of 1.94 has been calculated being consistent with the presence of Mn^{2+} in the structure [50,51].

Intermolecular hydrogen bonds with N–H···S distances of 2.5629(1) and 2.6185(1) Å (N–H···S angles: 161.485(2) – 174.264(3) °) and one S–H···S distance of 2.5850(1) Å (Table 3) connect the isolated complexes to form sheets within the *a*–*c* plane (Fig. 2).

The $[Mn(1,2\text{-chxn})_2SbS_3H]$ complexes form rods along the *b*-axis. Neighboured complexes are arranged in a face-to-face fashion along [1 0 0] and [0 0 1], i.e., the ligands are directed against each other (Fig. 3).

Compound **2** crystallizes in the orthorhombic space group *Pbca* (Table 1) with 4 formula units per unit cell. The Cr^{3+} ion is coordinated by four N atoms of the 1,3-dap ligand and by two S atoms of the $[SbS_3]^{3-}$ pyramid (Fig. 4) forming a distorted CrN_4S_2 octahedron.

The Cr–N and Cr–S bond lengths as well as the N–Cr–N/N–Cr–S angles are very similar to those of $[Cr(en)_2SbS_3]$, $[Cr(tren)_2SbS_3]$ and $[Cr(trien)_2SbS_3]$ (Table 4) [9,39,44]. The Cr–N(1) bond of 2.087(3) Å is slightly shorter then the other three Cr–N(2, 3, 4) distances (2.106(3) – 2.127(3) Å) which may be explained by steric constraints [9].

The geometric parameters of the $[SbS_3]^{3-}$ anion (Table 4) are typical for this building unit [9,39,44]. The terminal Sb–S(3) bond is as expected slightly shorter then the bridging Sb–S(1, 2) bonds. The next shortest contact between Sb and a S atom is at 3.9217(1) Å which is too long for bonding interactions.

The complexes are arranged in rods along the *a*- and *b*-axis. Two-dimensional sheets in the *a*–*c* plane are formed by intermolecular N–H···S bonds (2.4627(0) – 2.9190(1) Å; N–H···S

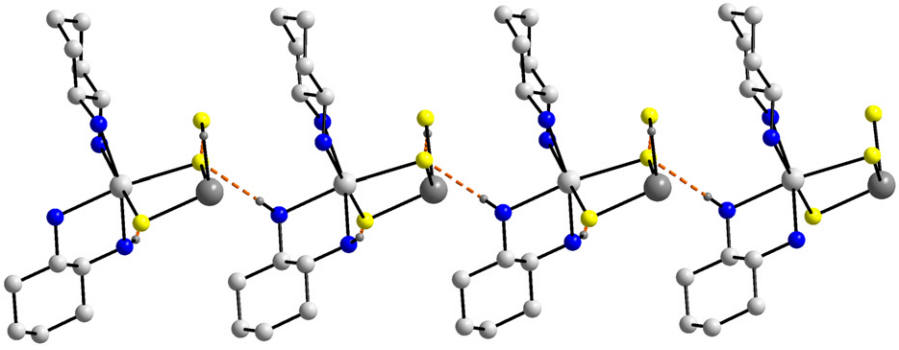

Fig. 2. Hydrogen bonding interactions in $[Mn(1,2\text{-chxn})_2SbS_3H]$ forming a sheet in the *a*–*c* plane (the hydrogen atoms which are not involved in S···H interactions are omitted for clarity).

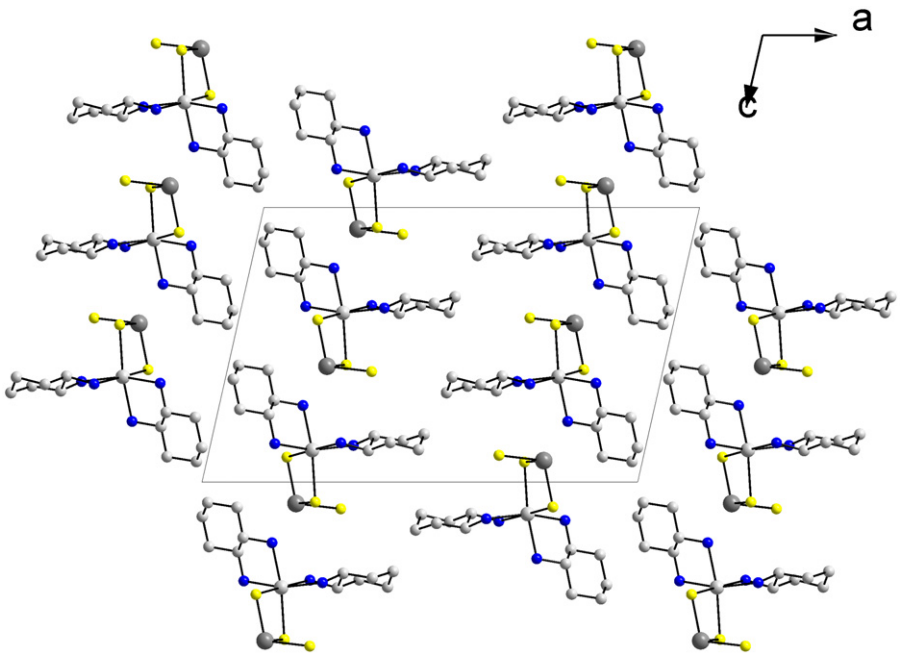

Fig. 3. Crystal packing of the $[Mn(1,2\text{-chxn})_2SbS_3H]$ complexes viewed along the *b*-axis.

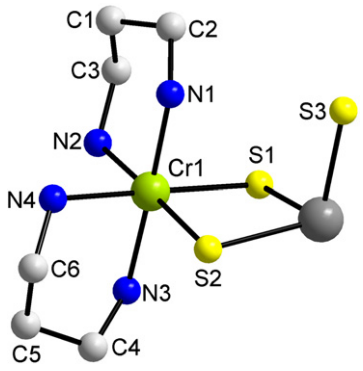

Fig. 4. The $[Cr(1,3\text{-dap})_2SbS_3]$ complex (the hydrogen atoms are omitted for clarity).

Table 4
Bond lengths (Å) and angles (°) for $[Cr(1,3\text{-dap})_2SbS_3]$ (2).

Sb(1)–S(1)	2.4375(10)	N(1)–Cr(1)–N(2)	91.66(13)
Sb(1)–S(2)	2.4086(11)	N(1)–Cr(1)–N(3)	178.09(14)
Sb(1)–S(3)	2.3664(12)	N(1)–Cr(1)–N(4)	90.20(13)
Cr(1)–N(1)	2.087(3)	N(1)–Cr(1)–S(1)	90.78(10)
Cr(1)–N(2)	2.106(3)	N(1)–Cr(1)–S(2)	90.02(10)
Cr(1)–N(3)	2.122(3)	N(2)–Cr(1)–N(3)	88.09(13)
Cr(1)–N(4)	2.127(3)	N(2)–Cr(1)–N(4)	89.60(14)
Cr(1)–S(1)	2.3942(11)	N(2)–Cr(1)–S(1)	89.83(10)
Cr(1)–S(2)	2.3582(11)	N(2)–Cr(1)–S(2)	178.29(10)
S(2)–Sb(1)–S(1)	88.28(3)	N(3)–Cr(1)–N(4)	87.91(14)
S(3)–Sb(1)–S(1)	103.55(4)	N(3)–Cr(1)–S(1)	91.12(11)
S(3)–Sb(1)–S(2)	100.43(4)	N(3)–Cr(1)–S(2)	90.22(10)
		N(4)–Cr(1)–S(1)	178.88(10)
		N(4)–Cr(1)–S(2)	90.05(10)
		S(2)–Cr(1)–S(1)	90.49(4)

angles: 150.76–173.0°) (Fig. 5, Table 5). Additionally, a strong intramolecular N–H–S bond between S(2) and H(1B) of 2.5649(1) Å (N–H···S angle: 167.168(1) °) is present in the complex.

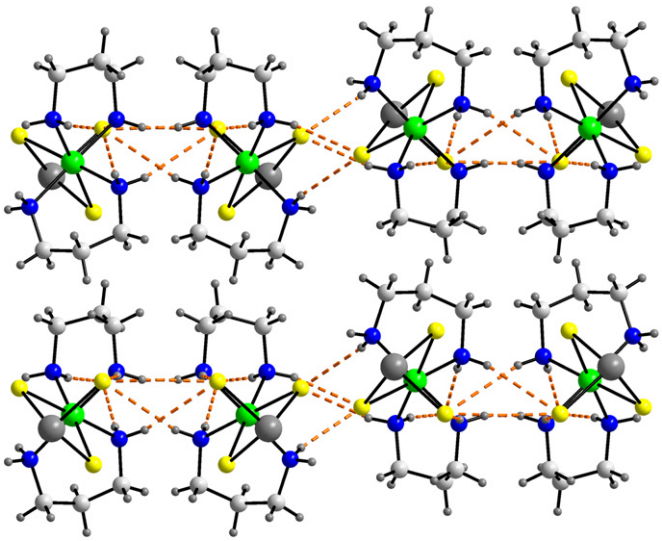

Fig. 5. $[Cr(1,3\text{-dap})_2SbS_3]$ molecules viewed along the *a*-axis and hydrogen bonds forming a sheet in the *a*–*c* plane.

Only one manganese thioantimonate containing 1,2-chxn as ligand is known besides **1** namely $[Mn(1,2\text{-chxn})_3]_2[Mn(1,2\text{-chxn}_2(Sb(V)S_4)_2]\ \Delta\ 6H_2O$ [34] and contains the $[Sb(V)S_4]^{3-}$ anion. The structure is constructed by two Mn^{2+} cations of which one is coordinated by three 1,2-chxn molecules and the second cation by two 1,2-chxn ligands and two monodentate $[SbS_4]^{3-}$ units leading to distorted octahedral environments. To the best of our knowledge no thioantimonate containing a Mn^{2+} cation coordinated by a $[SbS_3]^{3-}$ anion has been reported until now. This may be due to the fact that $[Mn(L)_2SbS_3]^-$ (L=organic ligand) carries a negative charge requiring an appropriate counterion. Indeed such charge compensation can be realized by a monoprotonated amine but in **1** the missing charge is compensated by a protonated sulphur atom. Such behaviour has not been reported for thioantimonates until now and it is not clear which synthetic conditions forces the formation of such protonated thioantimonates.

Table 5
Hydrogen bonds of $[Cr(1,3\text{-dap})_2SbS_3]$.

D–H		d(H…A)	< DHA/°
S1	H2A	2.6117(1)	160.796(1)
	H3A	2.6319(0)	150.755(1)
S2	H1A	2.4653(1)	163.514(1)
	H1B	2.5649(1)	167.168(1)
	H2B	2.4627(0)	169.318(1)
	H4A	2.9190(1)	166.085(1)
	H4B	2.7371(0)	173.004(1)

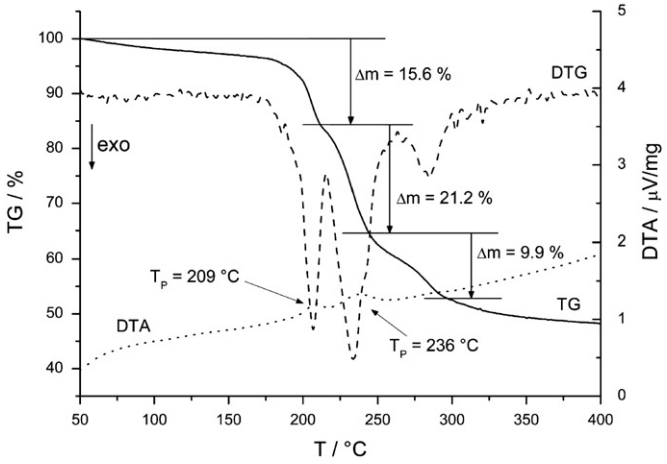

Fig. 6. TG-DTG curves of the thermal decomposition of $[Mn(1,2\text{-chxn})_2SbS_3H]$.

3.2. Thermal investigations

The DTA/TG curve of **1** is shown in Fig. 6. The compound decomposes in at least three steps (Δm=15.6, 21.2 and 9.9%) which are accompanied by endothermic signals. CHN analysis of the black residue reveals 6.6% of organic contamination (C: 5.37, H: 0.08 and N: 1.18%). In the X-ray powder pattern of the residue reflections of Sb and MnS_2 could be identified besides further peaks which cannot be explained. This observation is indicative for a very complex decomposition pattern involving redox reactions. Similar complex thermal decomposition reactions were also reported for $[Ni(aepa)_2]Sb_6S_{12}$ and $[Ni(aepa)_2]Sb_4S_7$ [52]. The TG/MS measurements of these two compounds show that the amine and fragments as well as H_2S are released during thermal degradation [52]. Hence a similar behavior can be expected for compound **1**.

The DTA/TG curve of **2** exhibits two mass losses (Δm=23.4 and 15.2%) being accompanied by two endothermic signals at T_P=291 (T_{Onset}=255 °C) and 342 °C (Fig. 7). The total weight loss is 38.6% and cannot be easily explained by the emission of e.g., two molecules 1,3-diaminopropane and one H_2S. In the grey residue a small contamination of 2.83% (C: 2.23, H: 0.06 and N: 0.54%) remains. The X-ray powder pattern of the residue is complex and only elemental Sb and $CrSbS_3$ could be identified.

3.3. Spectroscopy

In the Raman spectrum of **1** and **2** (Figs. 8 and 9) the bands at ca. 370 cm^{-1} can be assigned to the Sb–S stretching vibration. The S–Sb–S symmetric deformation vibration is located at 357 (**1**) and 349 cm^{-1} (**2**) while the resonances at 280 (**1**) and 294 cm^{-1} (**2**) are the S–Sb–S asymmetric stretching vibrations. At lower frequencies (148 (**1**) and 147 cm^{-1} (**2**)) the S–Sb–S symmetric

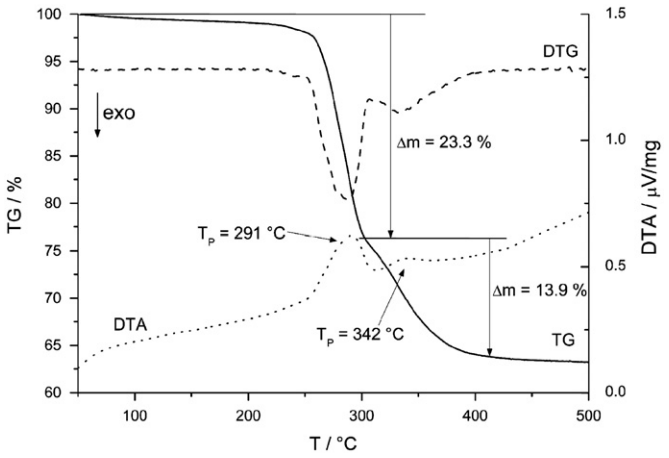

Fig. 7. DTA/TG curves of the thermal decomposition of $[Cr(1,3\text{-dap})_2SbS_3]$.

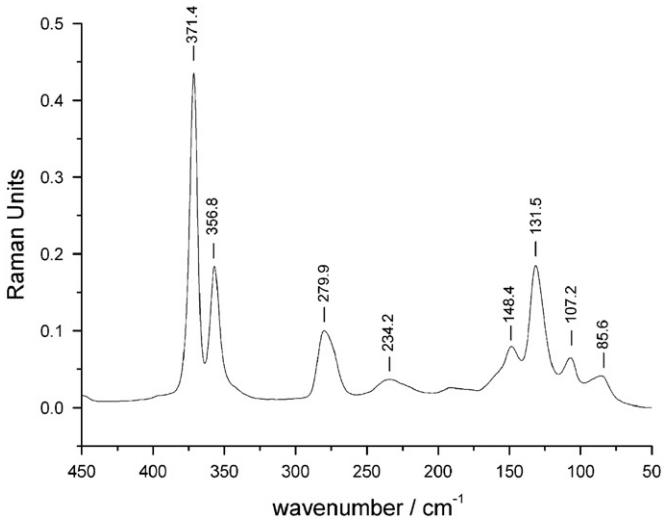

Fig. 8. Raman spectrum of $[Mn(1,2\text{-chxn})_2SbS_3H]$.

deformation vibration and the S–Sb–S symmetric bending vibration (107 cm^{-1}) occur [9]. Several other vibrations are seen which cannot be assigned unambiguously.

In the IR spectrum of compound 1 (Fig. 10) the absorptions located at 3421, 3315, 3298, 3286, 3199 and 3116 cm^{-1} could be assigned to the asymmetric and symmetric N–H stretching vibrations of the amino groups in 1,2-chxn (Fig. 10). The C–H stretching vibrations occur between 2960 and 2850 cm^{-1}. The N–H and C–H deformation modes are found at 1575 cm^{-1}, respectively 1445 cm^{-1}. The band located at 2464 cm^{-1} is assigned to the S(3)–H vibration [49].

3.4. Magnetic measurements

The temperature dependent inverse magnetic susceptibility of compound **1** is displayed in Fig. 11.

The paramagnetic behaviour of the compound over the whole temperature range is obvious from Fig. 11. Evaluation of the data between 20 and 180 °C applying the Curie-Weiss law results in an effective magnetic moment of about 5.5 μ_B/Mn^{2+} and is comparable with the spin only value of the d^5 electronic configuration of 5.92 μ_B/Mn^{2+}. The deviation from the spin only value may be caused by some impurities on the surface of the crystals. The value of the Weiss constant of about −1 K is negligible small indicating no exchange interactions between the molecules.

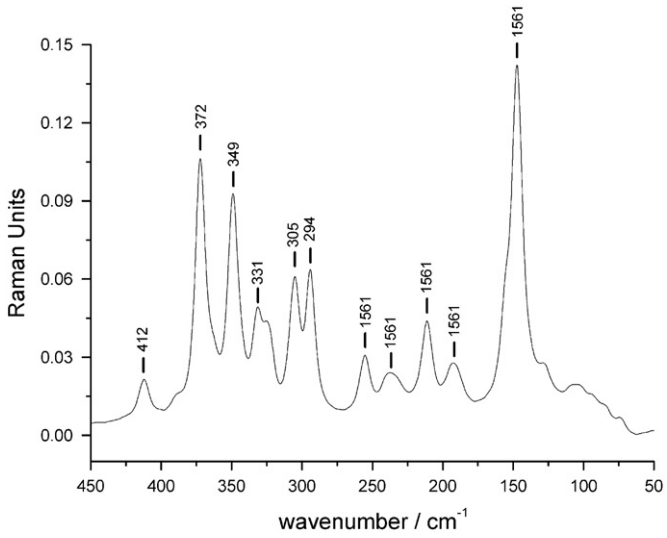

Fig. 9. Raman spectrum of $[Cr(1,3\text{-dap})_2SbS_3]$.

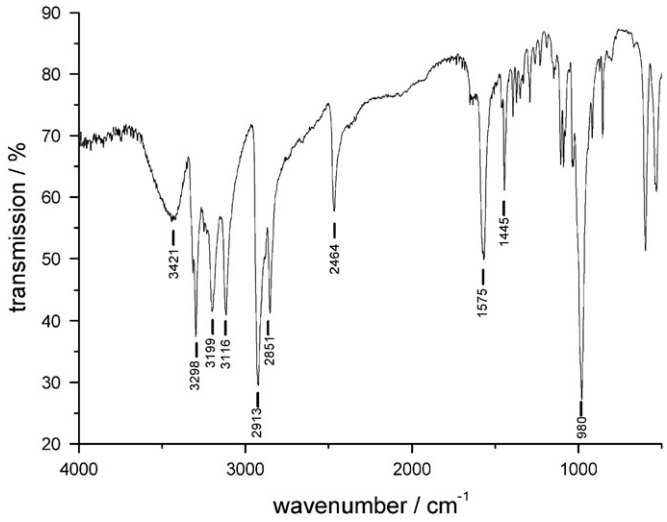

Fig. 10. IR spectrum of $[Mn(1,3\text{-dap})_2SbS_3H]$ with some prominent absorptions are marked.

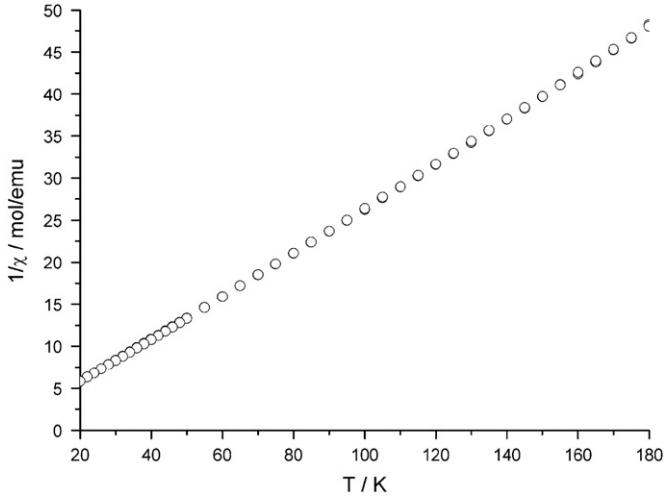

Fig. 11. Temperature dependence of the inverse magnetic susceptibility for $[Mn(1,2\text{-chxn})_2SbS_3H]$.

4. Summary

Until now most thioantimonates(III) with integrated transition metal cations were prepared with tetradentate ligands like tren or trien and only $[Cr(en)_2SbS_3]$ is formed with a bidentate amine as ligand. Neglecting the chalcophilic ions Cu^+ and Ag^+ there are only a few further exceptions like the Mn^{2+} containing thioantimonate networks with general composition $Mn_2(A)Sb_2S_5$ (A=1,3-dap, 1,3-dape, en, mdap, phen) (1,3-dape=1,3-diaminopentane, mdap=*N*-methyl-1,3-diaminopropane, phen=1,10-phenantroline) [14,31,33,36,38,53], $[Fe(trans\text{-}1,2\text{-chxn})_2Sb_6S_{10}]$ [16] or $[Co(en)_3]CoSb_4S_8$ [54]. Whereas in the topological similar chromium compounds $[Cr(en)_2SbS_3]$, $[Cr(tren)_2SbS_3]$, $[Cr(trien)_2SbS_3]$ and $[Cr(1,3\text{-dap})_2SbS_3]$ charge compensation is achieved by the Cr^{3+} cation, in $[Mn(1,2\text{-chxn})_2SbS_3H]$ charge neutrality is realized by a Mn^{2+} ion and a SH group. The compound $[Mn(1,2\text{-chxn})_2SbS_3H]$ represents the first example of a neutral Mn^{2+} complex with a bidentate amine and the bidentate acting $[SbS_3]^{3-}$ ligand. The successful isolation of the Mn^{2+} compound is another example highlighting the different chemical behavior of this cation compared to other first row transition metal ions. Whereas ions like Fe^{2+}, Co^{2+}, Ni^{2+} or Zn^{2+} prefer bonding to N atoms of the amines supplied in the reaction mixtures, Mn^{2+} seems to have a similar affinity to S and N atoms. We note that the compound $[Cr(1,3\text{-dap})_2SbS_3]$ is the second example for a Cr^{3+} containing isolated and neutral thioantimonate complex with a bidentate amine ligand. In both structures hydrogen bonding interactions interconnect the complexes into higher dimensional structures. Such S···H interactions are often observed in thiometalates and despite the low energy of a single S···H bond the large number of such bonds identified in **1** and **2** contribute to the stabilization of the compounds.

Acknowledgments

Financial support by the State Schleswig-Holstein and the Deutsche Forschungsgemeinschaft is gratefully acknowledged.

Appendix A. Supplementary material

Supplementary data associated with this article can be found in the online version at doi:10.1016/j.jssc.2012.01.013.

References

[1] H.A. Graf, H. Schäfer, Z. Naturforsch. 27b (1972) 735–739.
[2] H.A. Graf, H. Schäfer, Z. Anorg. Allg. Chem. 437 (1977) 183–187.
[3] H.A. Graf, H. Schäfer, Z. Anorg. Allg. Chem. 414 (1975) 211–219.
[4] H.A. Graf, H. Schäfer, Z. Anorg. Allg. Chem. 441 (1978) 93–97.
[5] H.A. Graf, H. Schäfer, Z. Anorg. Allg. Chem. 441 (1978) 98–102.
[6] B. Seidlhofer, N. Pienack, W. Bensch, Z. Naturforsch. 65b (2010) 937–975.
[7] A. Kromm, T. van Almsick, W.S. Sheldrick, Z. Naturforsch. 65b (2010) 918–936.
[8] J. Zhou, J. Dai, G.-Q. Bian, C.-Y. Li, Coord. Chem. Rev. 253 (2009) 1221–1247.
[9] K. Möller, C. Näther, W. Bensch, Z. Anorg. Allg. Chem. 633 (2007) 2635–2640.
[10] M. Schaefer, C. Näther, N. Lehnert, W. Bensch, Inorg. Chem. 43 (2004) 2914–2921.
[11] M. Schaefer, D. Kurowski, A. Pfitzner, C. Näther, Z. Rejai, K. Möller, N. Ziegler, W. Bensch, Inorg. Chem. 45 (2006) 3726–3731.
[12] H. Lühmann, Z. Rejai, K. Möller, P. Leisner, M.-E. Ordolff, C. Näther, W. Bensch, Z. Anorg. Allg. Chem. 634 (2008) 1687–1695.
[13] M. Schaefer, D. Kurowski, A. Pfitzner, C. Näther, W. Bensch, Acta Crystallogr. E60 (2004) m183–m185.
[14] A. Puls, C. Näther, W. Bensch, Z. Anorg. Allg. Chem. 632 (2006) 1239–1243.
[15] R. Stähler, C. Näther, W. Bensch, J. Solid State Chem. 174 (2003) (2003) 264–275.
[16] R. Kiebach, R. Warratz, C. Näther, W. Bensch, Z. Anorg. Allg. Chem. 635 (2009) 988–994.

[17] S. Lehmann, N. Pienack, H. Lühmann, M. El-Madani, C. Näther, W. Bensch, Z. Anorg. Allg. Chem. 634 (2008) 2323–2329.
[18] N. Pienack, C. Näther, W. Bensch, Z. Naturforsch. 63b (2008) 1243–1251.
[19] N. Pienack, K. Möller, C. Näther, W. Bensch, Solid State Sci. 9 (2007) 1110–1114.
[20] N. Pienack, C. Näther, W. Bensch, Eur. J. Inorg. Chem. (2009) 1575–1577.
[21] N. Pienack, A. Puls, C. Näther, W. Bensch, Inrog. Chem. 47 (2008) 9606–9611.
[22] N. Pienack, C. Näther, W. Bensch, Eur. J. Inorg. Chem. (2009) 937–946.
[23] M. Behrens, M.-E.- Ordolff, C. Näther, W. Bensch, K.-D.- Becker, C. Guillot-Deudon, A. Lafond, J.A. Cody, Inorg. Chem. 49 (2010) 8305–8309.
[24] V. Spetzler, H. Rijnberk, C. Näther, W. Bensch, Z. Anorg. Allg. Chem. 630 (2004) 142–148.
[25] V. Spetzler, C. Näther, W. Bensch, Inorg. Chem. 44 (2005) 5805–5812.
[26] A.V. Powell, S. Boissiere, A.M. Chippindale, Dalton Trans. (2000) 4192–4195.
[27] A.V. Powell, R. Paniagua, P. Vaqueiro, A.M. Chippindale, Chem. Mater. 14 (2002) 1220–1224.
[28] V. Spetzler, C. Näther, W. Bensch, Solid State Sci. 179 (2006) 3541–3549.
[29] A.V. Powell, J. Thun, A.M. Chippindale, J. Solid State Chem. 178 (2005) 3414–3419.
[30] P. Vaqueiro, A.M. Chippindale, A.R. Cowley, A.V. Powell, Inorg. Chem. 42 (2003) 7846–7851.
[31] W. Bensch, M. Schur, Eur. J. Solid State Inorg. Chem. 33 (1996) 1149–1160.
[32] M. Schur, C. Näther, W. Bensch, Z. Naturforsch. 56b (2001) 79–84.
[33] M. Schur, W. Bensch, Z. Naturforsch. 57b (2002) 1–7.
[34] M. Schaefer, L. Engelke, C. Näther, W. Bensch, Z. Anorg. Allg. Chem. 629 (2003) 1912–1918.
[35] M. Schaefer, C. Näther, W. Bensch, Solid State Sci. 5 (2003) 1135–1139.
[36] L. Engelke, R. Stähler, M. Schur, C. Näther, W. Bensch, R. Pöttgen, M.H. Möller, Z. Naturforsch. 59b (2004) 869–876.
[37] M. Schaefer, R. Stähler, W.-R. Kiebach, C. Näther, W. Bensch, Z. Anorg. Allg. Chem. 630 (2004) 1816–1822.
[38] X. Wang, T.-L. Sheng, S.-M. Hu, R.-B. Fu, X.-T. Wu, Inorg. Chem. Commun. 12 (2009) 399–401.
[39] M. Schur, H. Rijnberk, C. Näther, W. Bensch, Z. Anorg. Allg. Chem. 624 (1998) 2021–2024.
[40] R. Stähler, W. Bensch, Dalton Trans. (2001) 2518–2522.
[41] M. Schaefer, C. Näther, W. Bensch, Monatsh. Chem. 135 (2004) 461–470.
[42] E. Quiroga-Gonzales, C. Näther, W. Bensch, Solid State Sci. 12 (2010) 1235–1241.
[43] J. Lichte, H. Lühmann, C. Näther, W. Bensch, Z. Anorg. Allg. Chem. 635 (2009) 2021–2026.
[44] P. Vaqueiro, A.M. Chippindale, A.V. Powell, Polyhedron 22 (2003) 2839–2845.
[45] L. Engelke, C. Näther, P. Leisner, W. Bensch, Z. Anorg. Allg. Chem. 634 (2008) 2959–2965.
[46] R. Stähler, W. Bensch, Acta Crystallogr. C58 (2002) m537–m538.
[47] G.M. Sheldrick, SHELXS-97, Program for Crystal Structure Determination, University of Göttingen, Germany, 1997.
[48] G.M. Sheldrick, SHELXS-97, Program for the Refinement of Crystal Structures, University of Göttingen, Germany, 1997.
[49] M. Hesse, H. Meier, B. Zeeh, Spektroskopische Methoden in der Organischen Chemie, Thieme Georg Verlag, Stuttgart, 2002.
[50] O. Slupecki, I.D. Brown, Acta Crystallogr. B38 (1982) 1078–1079.
[51] W. Liu, H.H. Thorp, Inorg. Chem. 32 (1993) 4102–4105.
[52] B. Seidlhofer, J. Djamil, C. Näther, W. Bensch, Submitted to Cryst. Growth Des. 11 (2011) 5554–5560.
[53] D.-X. Jia, Y. Zhang, J. Dai, Q.-Y. Zhu, X.-M. Gua, J. Solid State Chem. 177 (2004) 2477–2483.
[54] H.-O. Stephan, M.G. Kanatzidis, J. Am. Chem. Soc. 118 (1996) 12226–12227.